

Monolithically integrated differential phase shift transmitter for quantum key distribution

H. O. Çirkinoglu¹, R. Santos², K. Williams¹, X. Leijtens¹

¹ Eindhoven University of Technology, 5612 AZ, Eindhoven, The Netherlands

² SMART Photonics, Eindhoven, The Netherlands

e-mail: h.o.cirkinoglu@tue.nl

ABSTRACT

An integrated differential phase shift QKD transmitter, which consist of a distributed Bragg reflector laser, a phase modulator, and Mach-Zehnder modulator sections for pulse carving and optical attenuation has been designed and fabricated. Initial characterization shows single mode operation of the laser with a linewidth around 2 MHz, and an achievable optical attenuation of more than 60 dB.

Keywords: Photonic Integrated Circuits, Quantum Key Distribution

1. INTRODUCTION

Quantum communication offers theoretically secure sharing of information through exploitation of the probabilistic nature of quantum physics [1]. Secure sharing of encryption keys can be guaranteed through quantum key distribution (QKD), without making any assumptions on how much computational power an eavesdropper might have [2]. Even though many successful quantum key distribution applications have been demonstrated [3, 4], many of them rely on bulk optics. Photonic integration offers realization of different optical functionalities on a single photonic chip; providing a platform for manufacturing scalable, robust, and mass-producible components for quantum key distribution applications. [5, 6]. Over more than three decades, there have been a number of protocols proposed for quantum key distribution, including BB84 [7], differential-phase shift (DPS) [8], and coherent-one-way (COW) [9]. In this work, we present an integrated DPS QKD transmitter, targeting the generation of weak pulses of phase-encoded optical coherent states. The fabrication of the chip is carried out through the generic platform of Smart Photonics [10, 11] as a part of the European Quantum Flagship project UNIQORN [12]. The fabricated transmitter consists of a distributed Bragg reflector (DBR) laser, an electro-refraction modulator to control the phase between pulses, a Mach-Zehnder Pulse carver to erase transition effects, and variable optical attenuator (VOA) stages to achieve the required signal levels. The security of the quantum channel is potentially compromised by the imperfect modulation of amplitude and phase of the transmitted signal [13]. We present the characterization results of the components of the chip, some of which were previously reported in [14]. We measured the laser spectrum and the laser linewidth, the dynamic response and the extinction ratio of the pulse carver, as well as the characteristics of the variable optical attenuator.

2. DIFFERENTIAL PHASE SHIFT QUANTUM KEY DISTRIBUTION

In DPS QKD using coherent light [15], the sender Alice prepares a pulse train of weak coherent states with average photon number of less than one, where the phase of each state is encoded randomly between $\{0, \pi\}$. The receiver Bob divides the received signal into two paths, and recombines them using a delay interferometer (DI) with a delay time equal to the time between each consecutive pulses. The DI is followed by photon detectors at its two outputs. The phase information at a time instance is retrieved based on which detector detects a photon. After transmission and detection, Bob reveals the information of the time instances at which a photon is detected. From this information, Alice can deduce what bit string Bob has. Compared to the well-known BB84 protocol, DPS QKD is advantageous due to the simplicity of detection, and utilization of each detected photon without the need of basis choice or sifting [16].

3. TRANSMITTER CHIP

The realized transmitter employs a light source consisting of a DBR laser [17] for light generation, an electro-refractive phase modulator section for phase encoding of the signal, and a Mach-Zehnder modulator (MZM) with electro-refractive modulators (ERM) in each of the interferometer arms for pulse carving. Multimode interference devices are used for splitting and combining of the signals. The transmitter is designed to be capable of switching between the classical and the quantum signal regime. In order to attain the required signal attenuation, the source is followed by a variable optical attenuator (VOA) function. For this, the circuit employs a cascade of three tunable Mach-Zehnder interferometers that can be tuned to each achieve up to 20 dB suppression. A schematic of the circuit, and a microscope image of the chip is shown in Fig. 1. The characterization results of the fabricated chips are presented below.

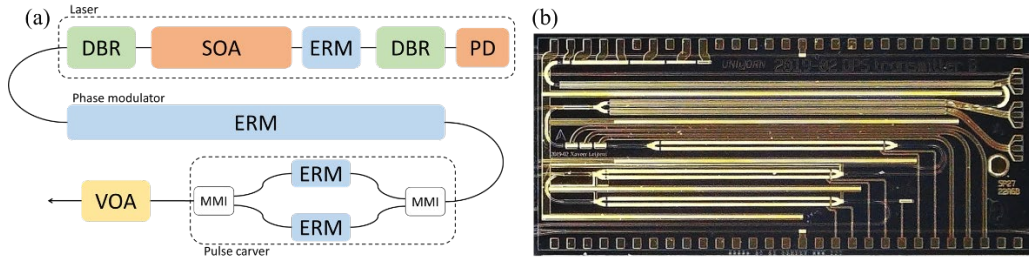


Figure 1. (a) The schematic of the DPS QKD transmitter chip, (b) Microscope image of the fabricated chip.

The DBR laser operates with a threshold current (I_{th}) of 28 mA at 22.1 °C, comparable to values for previously fabricated lasers with the same design [17]. The power of the light collected using a lensed fiber from an output waveguide after the pulse carver section is at around 0.5 mW for the SOA bias current of 100 mA.

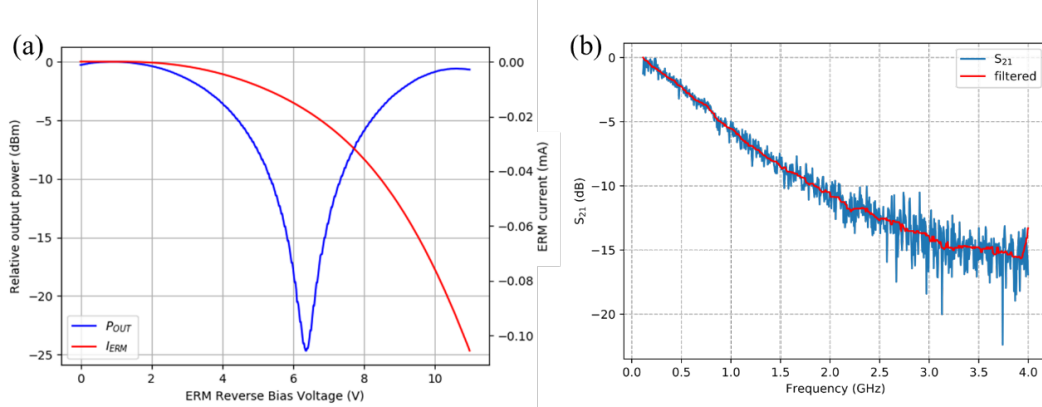


Figure 2. (a) The relative transmission of the first stage attenuator based on electro-refraction. (b) The dynamic response of the pulse carver

The attenuation of the output signal with the Mach-Zehnder-based VOA is evaluated. The output optical power, and the photo-current generated in the 2-mm-long active modulator section is recorded while varying the applied reverse bias voltage to one of the arms of the interferometer. The second arm is kept at a constant bias voltage. The response is given in Fig. 2(a). The figure shows a good extinction ratio of 24.6 dB, and a reverse bias voltage of 5.4 V is needed for π phase shift. The additional attenuation at 9.7 V bias voltage is at around 0.6 dB. The small signal response of the MZM pulse carver is measured using Agilent N4373C lightwave component analyser. The corresponding scattering parameter (S_{21}) is recorded for different speeds of the modulation signal applied to the MZM pulse carver. The resulting transmission characteristics (shown in blue), along with the trace (shown in red) obtained by applying a median filter to the acquired data is shown in Fig. 2(b), indicating a 3-dB cut-off point of around 590 MHz.

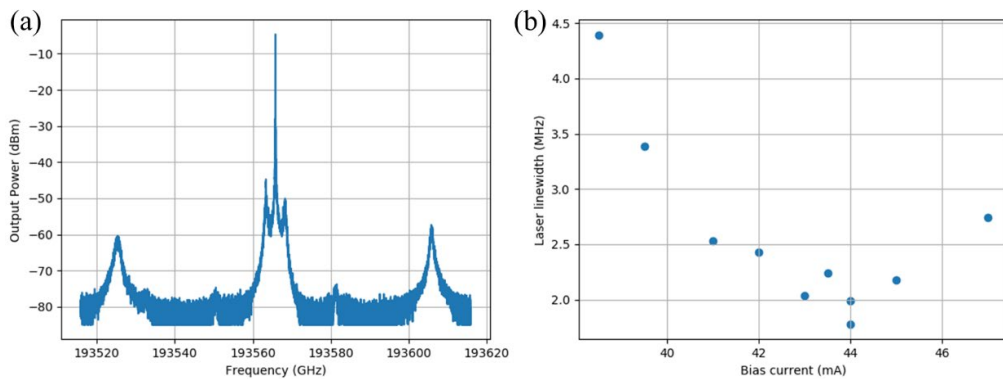


Figure 3. (a) Optical spectrum of the DBR laser (b) Linewidth measurement results for different bias current values

The optical spectrum, recorded by APEX 2041A spectrum analyzer with a resolution of 20 MHz is depicted in Fig. 3(a). The laser operating at 44 mA drive current results in a single mode emission around 1550 nm with >55 dB side-mode-suppression ratio. Two neighboring peaks around the main mode result from a relaxation oscillation frequency of around 3 GHz. The linewidth measurements for various bias current values are acquired using OEwaves OE4000 phase noise and linewidth measurement system, and are given in Fig. 3(b). The measurements display an intrinsic laser linewidth of ~ 2 MHz around 44 mA bias current. For 1 GHz modulation of the signal, a linewidth of 2 MHz corresponds to 0.2% of the receiver interferometer free-spectral-range, which results in a quantum bit error rate of $<0.5\%$ [13].

4.DISCUSSION

The tests carried out so far aimed to anticipate the suitability of the transmitter chip in a DPS QKD scheme, through the analysis of the performances of its individual components. Based on the data given in Fig 2(a), we expect to be able to achieve an attenuation of the signal by > 60 dB, with a three-stage MZM. The frequency response of the pulse carver indicate that the modulation rate of around 0.6 GHz is achievable. Generation of weak coherent states requires attenuation of the optical signal to a level of <1 photons per pulse, while maintaining a good optical signal-to-noise ratio. In our device, where the light source is integrated together with rest of the circuit, the signal suffers from a flat frequency noise, which originates from amplified spontaneous emission at the laser active region. Furthermore, the unguided stray light originating from spontaneous emission remains independent from the applied attenuation, decreasing the signal-to noise ratio as signal power is reduced. Our further planned investigations include the analysis of the transmitted signal in terms of single photon characteristics, followed by the verification of the transmitter in a DPS QKD testbed. In order to drive all required signals simultaneously for the desired operation, the samples will be wire-bonded and connectorized.

ACKNOWLEDGEMENTS

This work has received funding from the European Union's Horizon 2020 research and innovation programme through the Quantum-Flagship project UNIQORN under grant agreement No 820474. Nazca Design was used to generate the mask layout in this work.

REFERENCES

1. H.K. Lo, M. Curty, and K. Tamaki, "Secure quantum key distribution," *Nature Photonics*, vol. 8, 595-604, 2014.
2. V. Scarani, H. Bechmann-Pasquinucci, N.J. Cerf, M. Dušek, N. Lütkenhaus, and M. Peev, "The security of practical quantum key distribution," *Reviews of Modern Physics*, vol. 81, 1301-1350, 2009.
3. H. Takesue, E. Diamanti, T. Honjo, C. Langrock, M.M. Fejer, K. Inoue, and Y. Yamamoto, "Differential phase shift quantum key distribution experiment over 105 km fibre," *New Journal of Physics*, vol. 7, 232, 2005.
4. M. B. Costa e Silva, Q. Xu, S. Agnolini, P. Gallion, and F.J. Mendieta. "Homodyne detection for quantum key distribution: an alternative to photon counting in BB84 protocol" in *Proceedings of SPIE Photonics North*, vol. 6343, 63431R, 2006.
5. P. Sibson, C. Erven, M. Godfrey, S. Miki, T. Yamashita, M. Fujiwara, M. Sasaki, H. Terai, M.G. Tanner, C.M. Natarajan, R.H. Hadfield, J.L. O'Brien, and M.G. Thompson, "Chip-based quantum key distribution," *Nature Communications*, vol. 8, 13984, 2017.
6. P. Sibson, J.E. Kennard, S. Stanisic, C. Erven, J.L. O'Brien, and M.G. Thompson, "Integrated silicon photonics for high-speed quantum key distribution," *Optica*, vol. 4, 172-177, 2017.
7. C.H. Bennett, and G. Brassard, "Quantum public key distribution system," *IBM Technical Disclosure Bulletin*, vol. 28, 3153-3163, 1985.
8. K. Inoue, E. Waks, and Y. Yamamoto, "Differential phase shift quantum key distribution," *Physical Review Letters*, vol. 89, 037902, 2002.
9. D. Stucki, N. Brunner, N. Gisin, V. Scarani, and H. Zbinden, "Fast and simple one-way quantum key distribution," *Applied Physics Letters*, vol. 87, 194108, 2005.
10. Smit, Meint, et al, "An introduction to InP-based generic integration technology," *Semiconductor Science and Technology*, vol. 29.8, 083001, 2014.
11. "Smart Photonics", <http://smartphotonics.nl>.
12. "UNIQORN Project", <http://quantum-uniqorn.eu>.
13. T. Honjo, T. Inoue, and K. Inoue, "Influence of light source linewidth in differential-phase-shift quantum key distribution systems," *Optics Communications*, vol. 284, 5856-5859, 2011.
14. H.O. Çirkinoglu, R. Santos, K. Williams, and X. Leijtens, "An InP-based integrated modulated coherent state source for differential phase shift quantum key distribution," accepted for publication in 24th Annual Symposium of the IEEE Photonics Benelux Chapter, November 21-22, 2019, Amsterdam, Netherlands.
15. K. Inoue, E. Waks, and Y. Yamamoto. "Differential-phase-shift quantum key distribution using coherent light." *Physical Review A* vol. 68.2, 022317, 2003.
16. B. Schrenk, M. Hentschel, and H. Hübel. "Single-Laser Differential Phase Shift Transmitter for Small Form-Factor Quantum Key Distribution Optics." *Optical Fiber Communications Conference and Exposition (OFC), IEEE*, 1-3, 2018.
17. D. Zhao, "High-precision Distributed Bragg Reflectors in a Generic Photonics Integration Platform". PhD thesis, Eindhoven University of Technology, Eindhoven, The Netherlands, 2018. ISBN 978-90-386-4627-5.